Journal of Materials Chemistry B

RSC Publishing

PAPER

View Article Online
View Journal | View Issue

PEGylated denatured bovine serum albumin modified water-soluble inorganic nanocrystals as multifunctional drug delivery platforms†

Cite this: *J. Mater. Chem. B*, 2013, **1**, 1289

Liming Zhang,‡[ab] Zhuoxuan Lu,‡[ab] Yingying Bai,[c] Ting Wang,[a] Zhifei Wang,[a] Juan Chen,[a] Yin Ding,[d] Fei Yang,[a] Zhongdang Xiao,[a] Shenghong Ju,[c] Junjie Zhu[d] and Nongyue He*[a]

Received 7th November 2012
Accepted 7th January 2013

DOI: 10.1039/c2tb00380e

www.rsc.org/MaterialsB

A novel approach of using denatured bovine serum albumin (dBSA) to modify hydrophobic nanocrystals is reported. The dBSA layer outside of nanocrystals can adsorb water insoluble drugs excellently *via* hydrophobic interactions. Further PEGylation of the engineered nanocrystals greatly improves their aqueous stability. PEGylated dBSA modified upconversion nanoparticles, as a model for construction of integrating imaging and drug delivery platform, were also studied. The results demonstrated the modified upconversion nanoparticles not only maintain their unique up-conversion luminescence characters but also exhibit higher drug loading ability. Thus, such novel PEGylated dBSA modification approach expands the range of biological applications of inorganic nanocrystals.

Introduction

Inorganic nanocrystals become a new class of powerful materials for biological and medical applications such as sensing,[1–3] labeling,[2,4,5] optical imaging,[6–9] magnetic resonance imaging (MRI),[10,11] and hyperthermia,[12,13] because of their unique size-dependent optical, electronic, magnetic, and chemical properties. In the past decades, great progress has been achieved in the synthesis of inorganic nanocrystals with controlled sizes, shapes, and functionalized chemistry. The pyrolysis method has been widely used for preparing a wide variety of shape-controlled nanocrystals, such as Fe_3O_4 magnetic nanoparticles,[14,15] quantum dots (QDs),[16] and upconversion nanoparticles.[17] These nanocrystals usually are coated with non-polar molecules, enabling them to be well dispersed in non-polar solvent but difficult disperse in aqueous solution, which greatly limits their biomedical applications, especially for *in vivo* applications. Therefore, development of water-soluble nanocrystals with appropriate chemical modifications is an urgent issue for their application in biomedical fields.

Two common approaches have been exploited to modify inorganic nanocrystals to improve their water-solubility and biocompatibility.[2,18] The first approach uses different functional groups such as thiols, dithiols, phosphines, and dopamine derived PEG molecules to modify the surface of the nanocrystals *via* coordination bonds.[2,19] The other one uses amphiphilic molecules. The hydrophobic portion of amphiphilic molecules could bind with the hydrophobic molecules on the surface of the nanocrystals *via* hydrophobic interactions.[2,20] And then crystal micelles could be formed. Compared with the first approach, the second method using amphiphilic molecules has great advantages for expanding the functionality of the nanocrystals, particularly for loading hydrophobic drugs.[20]

Serum albumin is the most abundant plasma protein with a typical concentration of 50 mg mL^{-1} in the blood.[21] We recently reported that the denatured protein had a great ability to physically bind with hydrophobic drugs.[22] In this work, we firstly converted the amino group from bovine serum albumin (BSA) to a carboxyl group in order to increase the hydrophilicity of BSA. Then, we denatured the BSA as well to enhance its ability to bind with hydrophobic drugs. Very interestingly, the anchored denatured BSA (dBSA) not only maintains an excellent solubility in aqueous solution, but also effectively improves its solubility in some organic solvents, such as ethyl alcohol,

[a]*State Key Laboratory of Bioelectronics, School of Biological Science and Medical Engineering, Southeast University, Nanjing 210096, P. R. China. E-mail: nyhe1958@163.com*

[b]*Hunan Key Laboratory of Green Packaging and Application of Biological Nanotechnology, Hunan University of Technology, Zhuzhou 412008, P. R. China*

[c]*Department of Radiology & Molecular Imaging Laboratory, ZhongDa Hospital, Southeast University, Nanjing 210009, P.R. China*

[d]*State Key Laboratory of Analytical Chemistry for Life Science, Department of Chemistry, Nanjing University, Nanjing 210093, P. R. China*

† Electronic supplementary information (ESI) available: TEM images of nanocrystals; FT-IR spectra of dBSA coated nanocrystals; HDs of Fe_3O_4@dBSA–mPEG and Fe_3O_4@DMSA-dBSA–mPEG; photos of nanocrystals dispersed in 0.9% NaCl with and without 5% fetal bovine serum; and photos of nanocrystals dispersed in distilled water; photos of DOX unloaded or loaded Fe_3O_4@dBSA–mPEG nanoparticles solutions; fluorescence spectra (excitation at 980 nm) of $NaYF_4$:Yb,Er upconversion nanoparticles. See DOI: 10.1039/c2tb00380e

‡ Joint first authors, contributed equally to this work.

dimethylformamide (DMF), and dimethyl sulfoxide (DMSO), which makes it possible to use as-synthesized dBSA for direct modification of hydrophobic nanocrystals. And the engineered inorganic nanocrystals exhibit excellent adsorption ability for water insoluble drugs *via* hydrophobic interactions. Finally, further PEGylation of dBSA coated nanocrystals greatly improved the water solubility of the engineered nanocrystals. Our results demonstrate that the PEGylated dBSA modified nanocrystals exhibit excellent dispersion in aqueous solution. Thus engineered nanocrystals have great advantages for construction of multifunctional inorganic-nanocrystal-based drug delivery systems, and further expand the practical applications of the nanocrystals.

Considering the great importance of Fe_3O_4[23–25] and $NaYF_4$:Yb,Er upconversion nanocrystals[26,27] in biomedical imaging, we chose the above two types of hydrophobic nanocrystals as model systems for synthesis of water-soluble dBSA modified nanocrystal-based drug delivery systems. We also used PEGylated dBSA modified upconversion nanoparticles as a model to explore the feasibility of the engineered nanoparticles as multifunctional imaging and drug delivery platform. Through the study of drug loading behavior, and *in vitro* instantaneous imaging and drug delivery profile, we found these stable and multifunctional nanoparticles should have a wide range of potential applications in biomedical science and technology.

Results and discussion

Scheme 1 summarizes a novel route used to obtain water soluble and stable PEGylated dBSA modified inorganic nanocrystals. The oleic acid modified nanocrystals and dBSA was firstly mixed and stirred in chloroform and DMSO (V : V = 1 : 1) solution overnight. The supernatant was removed by centrifugation, and the nanocrystals were re-dispersed in DMSO solution. Then, dBSA modified nanocrystals were conjugated with amino-mPEG chemistry to further improve the water solubility. The resulting hydrophilic nanocrystals are highly soluble in aqueous solution contained salt and serum. As shown in Fig. 1, the sizes of the selected nanocrystals were showed as follows: oleic acid coated Fe_3O_4 (8 nm in diameter) and two different sizes of oleic acid coated $NaYF_4$:Yb,Er upconversion nanocrystals (85 and 170 nm in diameters, respectively).

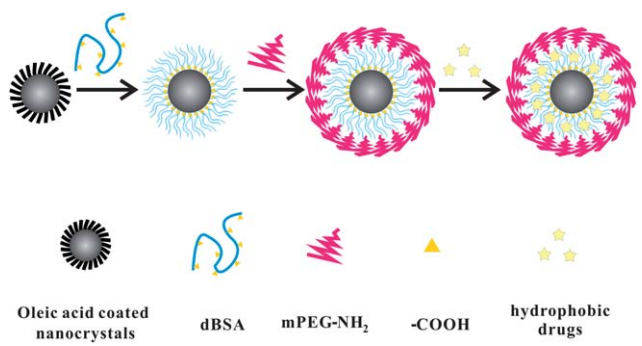

Scheme 1 Route for preparation of mPEGylated dBSA coated inorganic-nanocrystals-based drug delivery platforms.

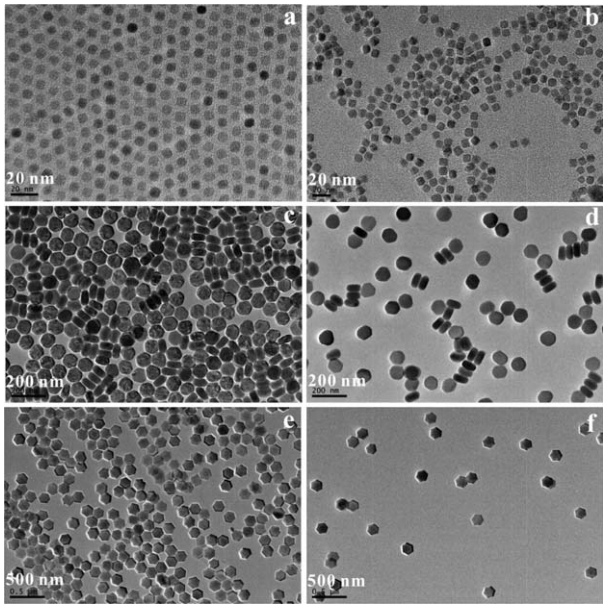

Fig. 1 TEM images of oleic acid (a) and PEGylated dBSA (b) coated Fe_3O_4, oleic acid coated 85 (c) and 170 nm (e) $NaYF_4$:Yb,Er nanocrystals, mPEG–dBSA coated 85 (d) and 170 nm (f) $NaYF_4$:Yb,Er nanocrystals.

TEM measurements show that dBSA and mPEG sequentially coated nanocrystals have almost identical sizes and shapes as compared with their oleic acid coated counterparts (Fig. 1). Upon negative staining with 1% phosphotungstic acid solution, about 1–2 nm thickness of organic layers is observed on the surface of the crystals, indicating the successful modification (see ESI, Fig. S1†). FT-IR spectra of the dBSA modified nanocrystals also show that the dBSA was successfully bonded with nanocrystals (see ESI, Fig. S2†). Broad peaks at ~1650 and ~2880 cm^{-1} are assigned to the vibration of amide and methylene groups, respectively. Dynamic light scattering (DLS) measurement demonstrates that the hydrodynamic diameters (HDs) of the nanocrystals are 94.4 nm with a PDI value of 0.251 for dBSA and mPEG sequentially coated Fe_3O_4 (Fe_3O_4@dBSA–mPEG), 139 nm with a PDI value of 0.163 and 239 nm with a PDI value of 0.352 for the two kinds of dBSA and mPEG sequentially coated $NaYF_4$:Yb,Er nanocrystals ($NaYF_4$:Yb,Er@dBSA–mPEG), respectively (Fig. 2a). The modified nanocrystal solutions show very low PDI values, suggesting excellent aqueous dispersion. The HDs measured by DLS are much larger than the diameters

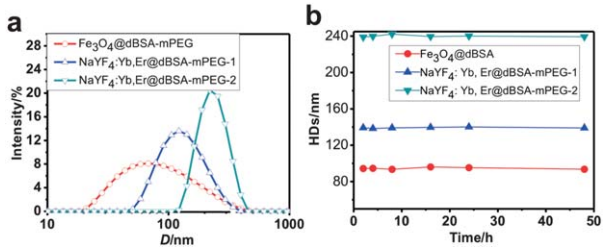

Fig. 2 HDs of the PEGylated dBSA coated nanocrystals (a) and stability of the nanocrystals (b).

measured by TEM. This is because the organic layers of the samples were dried and shrunken in size in the TEM measurement. Based on the above results, we speculate that the thickness of the mPEG–dBSA layer on the surface of the nanocrystals is 50–80 nm when the crystals are dispersed in the aqueous solution. Compared with the HDs of BSA (~10 nm),[22] the thickness of the mPEG–dBSA layer on the surface of the nanocrystals is much larger. Accordingly, we speculate that the thickness of the PEG hydration shell may be larger than 40 nm. In our previous research, we have confirmed that dBSA exhibits excellent adsorption ability for hydrophobic drugs *via* van der Waals interations.[22] Thus, the thick dBSA layer may give the nanocrystals new features to load hydrophobic drugs and constructing novel inorganic nanocrystal-based drug delivery platforms.

For oleic acid modified nanocrystals, the crystals can be coated with dBSA and then an mPEG layer using an optional method as follows: hydrophobic nanocrystals firstly transferred into hydrophilic nanocrystals by modification with dimercaptosuccinic acid (DMSA-nanocrystals).[28,29] The carboxyl groups in the dBSA were converted to amino groups by reaction with an excess amount of ethylenediamine. Then, aminated dBSA and mPEG–COOH were sequentially conjugated with DMSA-nanocrystals. It was reported that upon surface coating of DMSA-nanocrystals, the HDs of DMSA-Fe_3O_4 nanoparticles can be greatly enlarged to >200 nm, although the core size of Fe_3O_4 is only ~10 nm.[28] The HDs of Fe_3O_4@DMSA-dBSA–mPEG exhibit relative large sizes of 274 nm (see ESI, Fig. S3†), which is 2.8 times larger than that of Fe_3O_4@dBSA–mPEG. The nanocrystals with the larger size of 200 nm are not suitable for further *in vivo* application, because they could be rapidly removed by the reticuloendothelial system.[30]

For effective biomedical application of the nanocrystals, understanding of their stability under aqueous environments is critical. Accordingly, the stability of the PEGylated dBSA modified nanocrystals in an aqueous solution was also investigated. Fig. S4† shows the photos of modified nanocrystals dispersed in 0.9% NaCl solution with or without 5% serum. No precipitates in all tubes were seen after the solutions were placed for 24 h, suggesting excellent solubility of the modified nanocrystals. As shown in Fig. 2b, the HDs of synthesized nanocrystals did not obviously change in 48 h. In fact, no precipitates were observed after the nanocrystals were kept for even several months at 4 °C. However, the oleic acid coated nanocrystals are hardly dispersed in the water, and severe segregation was observed when they were dispersed in distilled water (see ESI, Fig. S5 and S6†), suggesting much higher water-dispersion of the mPEG–dBSA engineered nanocrystals.

We previously demonstrated that the dBSA did not show obvious cytotoxicity even at high concentration of 1 mg mL^{-1}.[22] In this study, cytotoxicity of the dBSA coated nanocrystals was measured by WST assay. Fig. 3a shows the cellular viability of the HeLa cells after the cells were incubated with different concentrations of PEGylated dBSA coated iron oxide and $NaYF_4$:Yb,Er nanocrystals. Over 90% relative cellular viability was detected for the engineered nanocrystals even at a rather high concentration (100 μg mL^{-1}), indicating that the cytotoxicity of these nanocrystals was ignorable. We next probe the drug delivery of these engineered crystals. In this strategy, mPEGylated dBSA coated $NaYF_4$:Yb,Er and Fe_3O_4 nanocrystals as models were tested for the drug adsorption. Anticancer drugs, doxorubicin (DOX), were incubated with $NaYF_4$:Yb,Er@dBSA–mPEG and Fe_3O_4@dBSA–mPEG in the PBS solution, and then DOX-loaded $NaYF_4$:Yb,Er@dBSA–mPEG complexes ($NaYF_4$:Yb,Er@dBSA–mPEG/DOX) and Fe_3O_4@dBSA–mPEG complexes (Fe_3O_4@mPEG–dBSA/DOX) were collected *via* centrifugation. As shown in Fig. 3c and S7,† the colors of the samples turned to red after the drugs were loaded. To confirm if DOX was actually loaded into the crystals, solutions of free DOX, $NaYF_4$:Yb,Er@dBSA–mPEG/DOX complexes and Fe_3O_4@mPEG–dBSA/DOX complexes were centrifuged for 20 min. Reddish precipitate and nearly colorless supernatant are observed upon centrifugation of the $NaYF_4$:Yb,Er@dBSA–mPEG/DOX complexes and Fe_3O_4@mPEG–dBSA/DOX complexes, while no obvious precipitate is noted for free DOX after centrifugation (Fig. 3c). These results clearly indicate that the DOX is successfully adsorbed to the mPEG–dBSA coated nanocrystals. UV-vis absorption spectra of the $NaYF_4$:Yb,Er@dBSA–mPEG/DOX complexes and Fe_3O_4@mPEG–dBSA/DOX complexes are also verified the successful adsorption of DOX, since obvious peak at ~490 nm (a characteristic peak of DOX[31,32]) is observed (Fig. 3b). The loading ratio of DOX (w/w, %) in the nanocrystals could be determined by the characteristic DOX absorption value at ~490 nm, Fig. 3d indicates that the drug loading ratio for

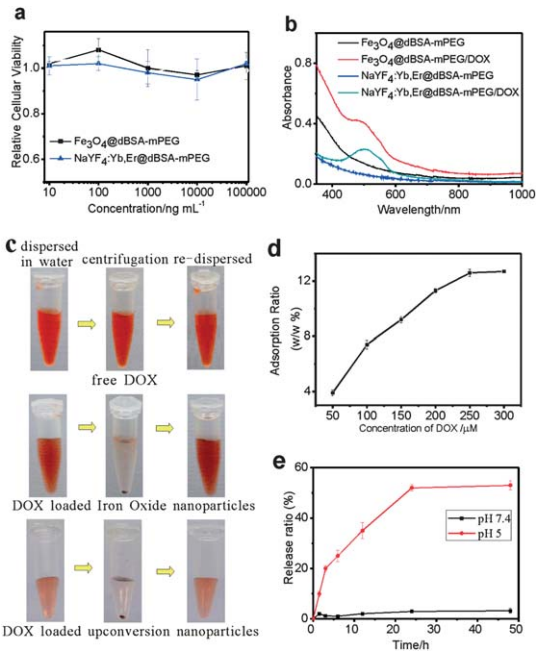

Fig. 3 Relative cellular viability of HeLa cells incubated with nanocrystals (a), UV-vis spectra of Fe_3O_4@dBSA–mPEG, $NaYF_4$:Yb,Er@dBSA–mPEG, DOX loaded Fe_3O_4@dBSA–mPEG complexes and DOX loaded NaYF4:Yb,Er@dBSA–mPEG (b), photos of free DOX, Fe_3O_4@dBSA–mPEG/DOX and $NaYF_4$:Yb,Er@dBSA–mPEG/DOX solutions after centrifugation and then sonication (c), loading ratio of DOX at different DOX concentrations. $NaYF_4$:Yb,Er@dBSA–mPEG solution maintains at same concentration (200 μg mL^{-1}) (d), DOX release ratio from $NaYF_4$:Yb,Er@dBSA–mPEG carriers over time in buffers at different pH values (e).

$NaYF_4$:Yb,Er@dBSA–mPEG was increased by increasing the DOX concentration from 50 to 250 μM, and maximum drug loading ratio is about 12.7%. The loading ratio is increased by ~50% in comparison with that of the C18PMH-PEG modified counterparts.[20] The drug loading ratio depends on the binding between the drug and hydrophobic regions of the amphiphilic molecules, and higher drug loading ratio of $NaYF_4$:Yb,Er@dBSA–mPEG in comparison with that modified by C18PMH-PEG may be ascribed to more hydrophobic regions existing in the dBSA molecules than in C18PMH.

Furthermore, for the drug release profile of DOX, pH 7.4 as well as acidic conditions (pH 5.0) was studied, since the normal pH of blood for sustaining human life is about 7.4, while the endosomes and lysosomes of cells are more acidic environments. The drug release study of the PEGylated dBSA modified nanoparticles was carried out in pH 7.4 and pH 5.0 phosphate buffer solutions, respectively. The released DOX concentrations from the nano-carriers were determined by UV-vis measurement of supernatants from $NaYF_4$:Yb,Er@dBSA–mPEG/DOX complexes after centrifugation at different time points. DOX released from the complexes at pH 7.4 was very minimal (less than 5%), while the maximum (~53% of DOX) was observed at pH 5.0 within 48 h (Fig. 3e). The protonation of the amino groups in the DOX increased its water-solubility, weakened its binding to the hydrophobic dBSA layer of the modified carriers, and finally triggered drug release.[20,31]

Upconversion nanoparticles absorb NIR photons and emit visible photons. Fluorescence imaging with upconversion nanoparticles has several advantages[26] over conventional fluorescence imaging, such as removal of auto fluorescence, deep penetration of NIR excitation and lower photodamage to living organisms. To demonstrate suitability of the as-modified upconversion nanoparticles for tissue imaging, we studied the changes of fluorescence spectra after the upconversion nanocrystals were modified with dBSA–mPEG. As illustrated in Fig. S8 (see ESI†), there is little change in the fluorescence spectra of modified and drug loaded upconversion nanoparticles. Excitation at 980 nm has been observed, suggesting sequential coating of dBSA and mPEG and then adsorbing of drugs did not change the natural optical properties of the upconversion nanoparticles. We next injected the nude mice with 100 μg of mPEG–dBSA modified upconversion nanoparticles in different depth of the tissues. Then, we traced the signal of the nanoparticles by using a modified *in vivo* Imaging System equipped with a 980 nm laser. As shown in Fig. 4a–d, high contrast images were captured wherever the nanoparticles were injected into the skin, muscle or deeper abdomen, suggesting the modified upconversion nanoparticles maintain their natural optical properties, and are suitable for bioimaging.

To further demonstrate the suitability of using the prepared water-soluble nanocrystals for multifunctional biomedical application, DOX loaded $NaYF_4$:Yb,Er nanocrystals, as a model, were explored for instantaneous cell imaging and drug delivery. To increase cellular enrichment of the nanocrystals, we use amine terminated 6-arm branched PEG, as an alternative to mPEG, conjugating with $NaYF_4$:Yb,Er@dBSA, which

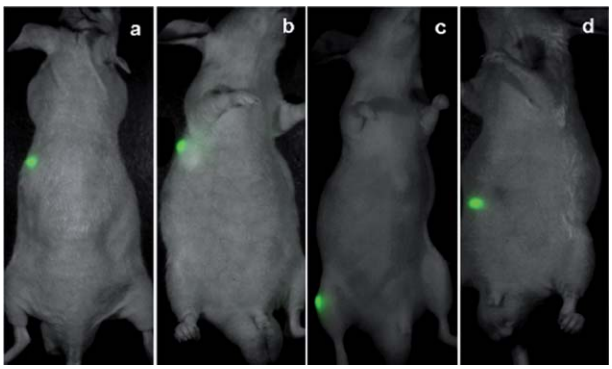

Fig. 4 Photos of *in vivo* upconversion luminescence animal imaging. $NaYF_4$:Yb,Er@dBSA–mPEG (100 μg) were injected into hypoderm (a and b), lag muscle (c) and abdomen (d) of nude mice.

yields amino-functionalized upconversion nanoparticles ($NaYF_4$:Yb,Er@dBSA-6-arm-PEG-NH_2). As shown in Fig. 5a, the diameter of the upconversion nanoparticles is ~50 nm, and their HD is 99.3 nm (data not shown). Folic acid, which specifically targets some cancer cells, such as HeLa cells and KB cells,[33,34] was next bound to the $NaYF_4$:Yb,Er@dBSA-6-arm-PEG-NH_2 *via* covalent conjugation between carboxyl groups of FA and amine groups of the nanocrystals ($NaYF_4$:Yb,Er@dBSA-6-arm-PEG-FA). Similar to the mPEG–dBSA coated nanocrystals, $NaYF_4$:Yb,Er@dBSA-6-arm-PEG-NH_2 shows excellent water solubility (Fig. 5b).

Because of the upconversion fluorescence signals from $NaYF_4$:Yb,Er nanocrystals (980 nm excitation) and down-conversion fluorescence from DOX (488 nm excitation), we can use a two-photon laser scanning fluorescence microscope to

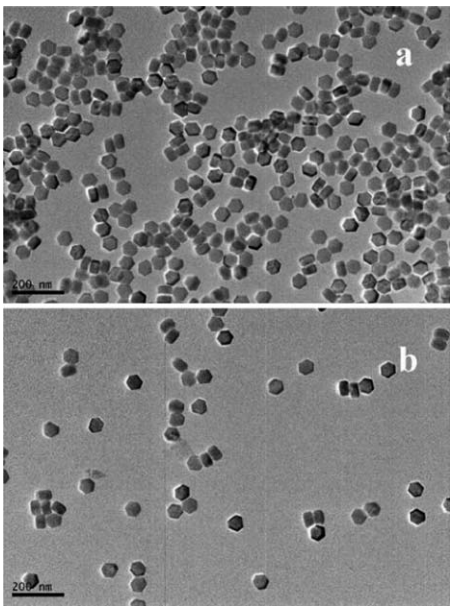

Fig. 5 TEM images of oleic acid coated $NaYF_4$:Yb,Er upconversion nanoparticles (a) and amine terminated 6-arm branched PEG-dBSA coated $NaYF_4$:Yb,Er with same magnification (b).

simultaneously capture the trace of upconversion nanoparticles and DOX. HeLa cells, FA receptor positive cell line, were incubated with $NaYF_4$:Yb,Er@dBSA-6-arm-PEG-NH_2/DOX complexes, $NaYF_4$:Yb,Er@dBSA-6-arm-PEG-FA/DOX complexes and free DOX for 4 h. From the fluorescence images, bright upconversion and downconversion photoluminescence were captured when the cells were incubated with DOX loaded FA modified upconversion nanoparticles, which strongly indicates the validity of these drug loaded upconversion nanoparticles as multifunctional imaging and drug delivery platforms. It should be noted that much weaker upconversion and downconversion photoluminescence could be detected when the cells were incubated with $NaYF_4$:Yb,Er@dBSA-6-arm-PEG/DOX complexes, strongly indicating that the conjugation of folic acid significantly increases the cellular uptake of the nano-carriers. Research on the imaging of FA-modified upconversion nanoparticles *in vivo* targeted molecular imaging is being conducted, and we believe these FA-modified nanoparticles will show good performance in *in vivo* imaging. As shown in Fig. 6, most upconversion fluorescence signal was captured in the cytoplasm, but most downconversion fluorescence signal was present in the nucleus, indicating the effective release of DOX from the complexes and then diffusion to the nucleus. These results suggest that the modified nanocrystal conjugates developed here are promising for many applications in biomedicine, including cell tracking and imaging-guided novel targeted cancer therapies.

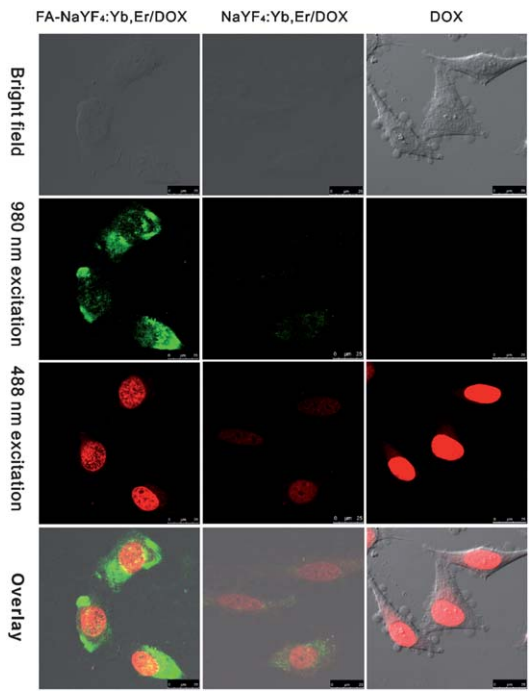

Fig. 6 Two-photon laser scanning fluorescence microscopy images of HeLa cells incubated with $NaYF_4$:Yb,Er@dBSA-6-arm-PEG-FA/DOX (a), $NaYF_4$:Yb,Er@dBSA-6-arm-PEG/DOX complexes (b) and free DOX (c) for 4 h. UCL emissions (green color) and DOX fluorescence (red color) were recorded in the wavelength ranges of 520–560 nm and 560–600 nm, under 980 nm and 488 nm laser excitation, respectively. All images were taken under identical instrumental conditions.

Conclusions

In summary, we have successfully established a novel approach for using dBSA to modify hydrophobic nanocrystals, which can be used for novel multifunctional drug delivery platforms. The novel synthesized nanocrystals exhibit excellent performance properties including high stability in aqueous solutions and non-toxicity. Moreover, compared with their other amphiphilic molecule modified counterparts, the PEGylated dBSA modified nanocrystals show highly efficient adsorption performance of hydrophobic drugs. Both of these advantages expand the range of biological applications available for these nanocrystals. Thus, our work opens a door for modification of nanocrystals and construction of multifunctional drug delivery platforms. Future work will be focused on *in vivo* distribution and toxicity, especially immunity of the modified nanocrystals, and developing applications of these promising materials.

Experimental section

Materials

Bovine serum albumin (BSA) and doxroubicin hydrochloride (DOX) were purchased from Sangon, China. Amine terminated PEG was ordered from Yarebio. Co. Ltd., Shanghai. Octadecene (ODE), $YbCl_3$, YCl_3, and $ErCl_3$ were purchased from Sigma-Aldrich. Other chemicals were purchased from Sinopharm Chemicals Reagent Co. Ltd. (China).

Characterization

The morphologies and sizes of nanoparticles were characterized using a JEM-2100 TEM microscope, and DLS analysis was performed with a Marlven Zetasizer Nano S90. *In vitro* cell fluorescence images were obtained with a Leica TCS SP5 confocal laser scanning microscope. Upconversion fluorescent spectra were recorded with a Hitachi F-4600 fluorescence spectrophotometer attached to an external 980 nm laser diode (Nanjing Lai-chuang Laser Ltd, China) instead of an internal Xe lamp. FT-IR spectra were collected by using a Thermo Nicolet 6700 FTIR spectrometer. UV-vis spectral measurements were taken on a Perkin Elmer Lambda 25 spectrophotometer. Absorbance in WST assay was read by Biotek Elx 800 Microplate Reader. Cell lines were cultured with a Water-Jacketed CO_2 Incubator (Thermo 3111).

Synthesis of denatured bovine serum albumin

BSA (1 g) was dissolved in 20 mL of distilled water, followed by adding excess succinic acid (2.36 g, 20 mmol). Then, the pH value of the solution was adjusted to 7 using triethylamine under vigorous stirring. Finally, 1-ethyl-3-[3-dimethylaminopropyl]carbodiimide hydrochloride (EDC) (0.955 g, 5 mmol) was added and the solution was stirred for 1 h. The resultant solution was then heated to 85 °C and incubated for 1 h. After the solution was cooled down to room temperature, EDC (0.955 g, 5 mmol) was again added, and the solution was stirred overnight. The resultant solution was purified *via* dialysis against distilled water for at least 72 h, and the products were obtained by vacuum freeze-drying.

Synthesis of oleic acid coated Fe_3O_4, $NaYF_4$:Yb,Er upconversion nanocrystals

Oleic acid coated Fe_3O_4 and $NaYF_4$:Yb,Er upconversion nanocrystals were synthesised according to previous literature.[17,29,35,36]

Preparation of dBSA and mPEG sequentially coated Fe_3O_4 or $NaYF_4$:Yb,Er nanocrystals

Fe_3O_4 or $NaYF_4$:Yb,Er nanocrystals (10 mg) were dispersed in chloroform, and dBSA (50 mg in 10 mL of DMSO) was rapidly added into the reaction solution under vigorous stirring, and kept stirr overnight. The dBSA modified nanocrystals were collected by centrifugation at 13 000 rpm. For further PEG modification, the dBSA coated nanocrystals were dispersed in 10 mL of DMSO. Then, 100 mg of $mPEG_{5000}$–NH_2 was added and stirred for 30 min to form a homogeneous solution. Finally, EDC (95.5 mg, 0.5 mmol) was added and the solution was stirred overnight. The modified nanocrystals were collected and washed with distilled water by centrifugation at 13 000 rpm. And the final products were dispersed in distilled water and filtered with a 220 nm filter.

Cell culture

HeLa cells were maintained in RPMI 1640 medium supplemented with 10% fetal bovine serum (FBS). Cells were seeded in tissue culture flasks (about 3×10^5 cells) and incubated in a fully humidified atmosphere at 37 °C with 5% CO_2. For cellular uptake tracking of $NaYF_4$:Yb,Er@dBSA–mPEG, the cells were seeded in 24-well plates at a density of about 1×10^4 cells per well in culture medium (0.5 mL) and maintained for 24 h. For cytotoxicity assays, the cells were seeded in 96-well plates at a density of 3×10^3 cells per well in medium (200 μL) and maintained for 24 h.

Measurement of relative cellular viability by WST assay

WST assays[31,32] were performed to evaluate the cytotoxicity of mPEGylated dBSA coated nanocrystals at different concentrations. In brief, HeLa cells were seeded in 96-well plates, and incubated with the nanocrystals for 24 h, and washed with PBS buffer. The relative cellular viability was checked by the WST assay. The data are presented as the mean ± standard deviation.

Loading and release of doxorubicin

DOX loading onto Fe_3O_4@dBSA–mPEG and $NaYF_4$:Yb,Er@dBSA–mPEG nanocrystals were done by mixing DOX (100 μM) with the nanocrystals (0.2 mg mL^{-1}) in phosphate buffer solution at 25 °C (PBS, pH 8.0, 20 mM) overnight. And free DOX was removed by centrifugation at 13 000 rpm for 10 min. The supernatant was discarded and the complexes were re-suspended and sonicated in PBS buffer to form a homogeneous solution and stored at 4 °C. The DOX loading ratio for PEGylated dBSA coated $NaYF_4$:Yb,Er nanoparticles was estimated from the absorbance at 490 nm, in the UV-vis spectra, after subtracting the absorbance from the nanocrystals.

The release of DOX from upconversion nanocrystals was performed by adding them to 0.1 M PBS buffer at 25 °C and different pH values (5.0 and 7.4, respectively). After incubation for the programmed time, the mixture was centrifuged, and supernatants were preserved for measurement of the released DOX.

In vivo imaging of $NaYF_4$:Yb,Er@dBSA–mPEG

Nude mice were chosen for *in vivo* studies. The $NaYF_4$:Yb,Er@dBSA–mPEG (100 μg were injected subcutaneously in the back, deeper upper leg muscle and abdomen. Upconversion luminescence was observed and images were captured by excitation with a 980 nm laser and recorded using an *in vivo* Imaging System.

Preparation of folic acid modified $NaYF_4$:Yb,Er nanoparticles

$NaYF_4$:Yb,Er nanocrystals (10 mg) were dispersed in chloroform, and dBSA (50 mg in 10 mL of DMSO) was rapidly added into the reaction solution under vigorous stirring, and kept stirring overnight. The dBSA modified nanocrystals were collected by centrifugation at 13 000 rpm. For further PEG modification, the dBSA coated nanocrystals were dispersed in 10 mL of DMSO. Then, 100 mg of amine terminated 6-arm PEG (MW 10 K) was added and kept stirring for 30 min to form homogeneous solution. Finally, EDC (95.5 mg, 0.5 mmol) was added and the solution was stirred overnight. The 6-arm-PEGylated dBSA coated nanocrystals were collected and washed with distilled water by centrifugation at 13 000 rpm. And the final products were dispersed in distilled water and filtered with a 220 nm filter. For folic acid functionalization, 10 mg of folic acid were dissolved in 1% $NaHCO_3$ solution, and added into the 6-arm-PEGylated dBSA coated nanocrystals solution. The mixture was sonicated for 10 min, and EDC was added to obtain the concentration of 0.1 mM mL^{-1}. Then, the mixture was kept stirring for overnight, The FA-6-arm-PEGylated dBSA coated nanocrystals were collected and washed with 1% $NaHCO_3$ by centrifugation at 13 000 rpm.

Targeted cellular uptake of DOX loaded $NaYF_4$:Yb,Er@dBSA-6-arm-PEG-FA

Cellular uptake of DOX loaded $NaYF_4$:Yb,Er@dBSA-6-arm-PEG-NH_2, DOX loaded $NaYF_4$:Yb,Er@dBSA-6-arm-PEG-FA, and free DOX (~100 and 10 μg mL^{-1}, calculated by $NaYF_4$:Yb,Er@dBSA-6-arm-PEG and DOX, respectively) was incubated with HeLa cells for 4 h and washed with PBS buffer 3 times. The fluorescence images were captured with a confocal laser scanning microscope.

Acknowledgements

This work was supported by 973 Project (no. 2010CB933903), NSFC (no. 61271056 and no. 21205036), Hunan Provincial Natural Science Foundation of China (no. 12JJ4049), and the Open Research Fund of State Key Laboratory of Bioelectronics, Southeast University. China Postdoctoral Science Foundation funded projects (no. 2012M511660 and no. 2012M520981).

Notes and references

1 J. Liu and Y. Lu, *Angew. Chem.*, 2006, **118**, 96–100.
2 I. L. Medintz, H. T. Uyeda, E. R. Goldman and H. Mattoussi, *Nat. Mater.*, 2005, **4**, 435–446.
3 R. Elghanian, J. J. Storhoff, R. C. Mucic, R. L. Letsinger and C. A. Mirkin, *Science*, 1997, **277**, 1078–1081.
4 J. Shan, Z. Yong, L. Kian Meng, K. W. S. Eugene and Y. Lei, *Nanotechnology*, 2009, **20**, 155101.
5 X. Wu, H. Liu, J. Liu, K. N. Haley, J. A. Treadway, J. P. Larson, N. Ge, F. Peale and M. P. Bruchez, *Nat. Biotechnol.*, 2003, **21**, 41–46.
6 M. Wang, C.-C. Mi, W.-X. Wang, C.-H. Liu, Y.-F. Wu, Z.-R. Xu, C.-B. Mao and S.-K. Xu, *ACS Nano*, 2009, **3**, 1580–1586.
7 X. Yu, M. Li, M. Xie, L. Chen, Y. Li and Q. Wang, *Nano Res.*, 2010, **3**, 51–60.
8 L. Cheng, K. Yang, Y. Li, J. Chen, C. Wang, M. Shao, S.-T. Lee and Z. Liu, *Angew. Chem., Int. Ed.*, 2011, **50**, 7385–7390.
9 D. H. Dam, J. H. Lee, P. N. Sisco, D. T. Co, M. Zhang, M. R. Wasielewski and T. W. Odom, *ACS Nano*, 2012, **6**, 3318–3326.
10 J. Chomoucka, J. Drbohlavova, D. Huska, V. Adam, R. Kizek and J. Hubalek, *Pharmacol. Res.*, 2010, **62**, 144–149.
11 G. Mikhaylov, U. Mikac, A. A. Magaeva, V. I. Itin, E. P. Naiden, I. Psakhye, L. Babes, T. Reinheckel, C. Peters, R. Zeiser, M. Bogyo, V. Turk, S. G. Psakhye, B. Turk and O. Vasiljeva, *Nat. Nanotechnol.*, 2011, **6**, 594–602.
12 C. Wang, J. Chen, T. Talavage and J. Irudayaraj, *Angew. Chem., Int. Ed.*, 2009, **48**, 2759–2763.
13 Z. Zhang, L. Wang, J. Wang, X. Jiang, X. Li, Z. Hu, Y. Ji, X. Wu and C. Chen, *Adv. Mater.*, 2012, **24**, 1349.
14 W. S. Chiu, S. Radiman, M. H. Abdullah, P. S. Khiew, N. M. Huang and R. Abd-Shukor, *Mater. Chem. Phys.*, 2007, **106**, 231–235.
15 J. Park, E. Lee, N.-M. Hwang, M. Kang, S. C. Kim, Y. Hwang, J.-G. Park, H.-J. Noh, J.-Y. Kim, J.-H. Park and T. Hyeon, *Angew. Chem.*, 2005, **117**, 2932–2937.
16 B. O. Dabbousi, J. Rodriguez-Viejo, F. V. Mikulec, J. R. Heine, H. Mattoussi, R. Ober, K. F. Jensen and M. G. Bawendi, *J. Phys. Chem. B*, 1997, **101**, 9463–9475.
17 H.-S. Qian and Y. Zhang, *Langmuir*, 2008, **24**, 12123–12125.
18 H. Wu, H. Zhu, J. Zhuang, S. Yang, C. Liu and Y. C. Cao, *Angew. Chem., Int. Ed.*, 2008, **47**, 3730–3734.
19 J.-C. Boyer, M.-P. Manseau, J. I. Murray and F. C. J. M. van Veggel, *Langmuir*, 2009, **26**, 1157–1164.
20 C. Wang, L. Cheng and Z. Liu, *Biomaterials*, 2011, **32**, 1110–1120.
21 T. Peters, Jr, *Adv. Protein Chem.*, 1985, **37**, 161–245.
22 L. Zhang, Z. Lu, X. Li, Y. Deng, F. Zhang, C. Ma and N. He, *Polym. Chem.*, 2012, **3**, 1958–1961.
23 J. Kim, J. E. Lee, S. H. Lee, J. H. Yu, J. H. Lee, T. G. Park and T. Hyeon, *Adv. Mater.*, 2008, **20**, 478–483.
24 J. Xie, C. Xu, N. Kohler, Y. Hou and S. Sun, *Adv. Mater.*, 2007, **19**, 3163–3166.
25 Y. Pan, M. J. C. Long, H.-c. Lin, L. Hedstrom and B. Xu, *Chem. Sci.*, 2012, **3**, 3459–3499.
26 Y. I. Park, J. H. Kim, K. T. Lee, K.-S. Jeon, H. B. Na, J. H. Yu, H. M. Kim, N. Lee, S. H. Choi, S.-I. Baik, H. Kim, S. P. Park, B.-J. Park, Y. W. Kim, S. H. Lee, S.-Y. Yoon, I. C. Song, W. K. Moon, Y. D. Suh and T. Hyeon, *Adv. Mater.*, 2009, **21**, 4467–4471.
27 G. Tian, Z. Gu, L. Zhou, W. Yin, X. Liu, L. Yan, S. Jin, W. Ren, G. Xing, S. Li and Y. Zhao, *Adv. Mater.*, 2012, **24**, 1226–1231.
28 Z. P. Chen, Y. Zhang, S. Zhang, J. G. Xia, J. W. Liu, K. Xu and N. Gu, *Colloids Surf., A*, 2008, **316**, 210–216.
29 Q. Chen, X. Wang, F. Chen, Q. Zhang, B. Dong, H. Yang, G. Liu and Y. Zhu, *J. Mater. Chem.*, 2011, **21**, 7661–7667.
30 L. Brannon-Peppas and J. O. Blanchette, *Adv. Drug Delivery Rev.*, 2004, **56**, 1649–1659.
31 L. Zhang, J. Xia, Q. Zhao, L. Liu and Z. Zhang, *Small*, 2010, **6**, 537–544.
32 L. Zhang, Z. Lu, Q. Zhao, J. Huang, H. Shen and Z. Zhang, *Small*, 2011, **7**, 460–464.
33 X. Wang, A. R. Morales, T. Urakami, L. Zhang, M. V. Bondar, M. Komatsu and K. D. Belfield, *Bioconjugate Chem.*, 2011, **22**, 1438–1450.
34 D. J. Bharali, D. W. Lucey, H. Jayakumar, H. E. Pudavar and P. N. Prasad, *J. Am. Chem. Soc.*, 2005, **127**, 11364–11371.
35 J. Park, K. An, Y. Hwang, J.-G. Park, H.-J. Noh, J.-Y. Kim, J.-H. Park, N.-M. Hwang and T. Hyeon, *Nat. Mater.*, 2004, **3**, 891–895.
36 T. K. Sau and C. J. Murphy, *Langmuir*, 2004, **20**, 6414–6420.